

ABM11 parton distributions and benchmarks

Sergey Alekhin^{1,2}, Johannes Blümlein¹, Sven-Olaf Moch¹

¹DESY, Platanenallee 6, D-15738 Zeuthen, Germany

²Institute for High Energy Physics, 142281 Protvino, Moscow region, Russia

DOI: will be assigned

We present a determination of the nucleon parton distribution functions (PDFs) and of the strong coupling constant α_s at next-to-next-to-leading order (NNLO) in QCD based on the world data for deep-inelastic scattering and the fixed-target data for the Drell-Yan process. The analysis is performed in the fixed-flavor number scheme for $n_f = 3, 4, 5$ and uses the \overline{MS} scheme for α_s and the heavy quark masses. The fit results are compared with other PDFs and used to compute the benchmark cross sections at hadron colliders to the NNLO accuracy.

The nucleon PDFs play crucial role in the collider phenomenology and very often they put a limit on theoretical prediction accuracy, particularly for the calculations in the next-to-next-to-leading order (NNLO) in QCD. To meet quick accumulation of the data and steady progress in reduction of the systematic uncertainties in the LHC experiment we provide the NNLO nucleon PDF set with improved accuracy [5]. These PDFs are obtained from the updated version of the ABKM09 analysis [6] performed in the fixed-flavor number (FFN) scheme with the number of fermions taken as $n_f = 3, 4, 5$, depending on the process used to constrain the PDFs. In the present analysis we replace the inclusive neutral-current (NC) DIS data of the H1 and ZEUS experiments by the combined HERA data set, which are obtained from merging those of separate experiments [7]. The data are substantially improved by cross-calibration of the separate experiments and by merging both statistical and systematic errors. Due to these improvements the combined HERA data provide a better constraint on the small- x gluon and quark distributions. We also add to our analysis the inclusive charged-current (CC) DIS HERA data obtained by merging the H1 and ZEUS samples. The CC HERA data provide a supplementary constraint on the PDFs helping to disentangle the small- x quark distributions. Finally, we include the H1 data obtained in a spe-

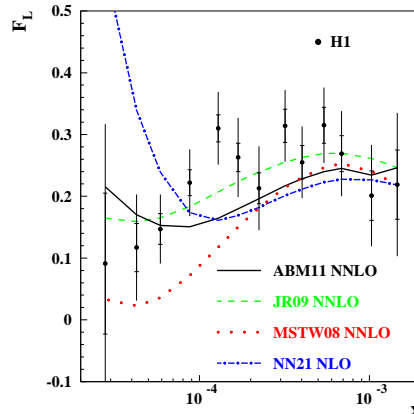


Figure 1: The data on F_L versus x obtained by the H1 collaboration [1] confronted with the 3-flavor scheme NNLO predictions based on the different PDFs (solid line: this analysis, dashes: JR09 [2], dots: MSTW [3]). The NLO predictions based on the 3-flavor NN21 PDFs [4] are given for comparison (dashed dots). The value of Q^2 for the data points and the curves in the plot rises with x in the range of $1.5 \div 45 \text{ GeV}^2$.

cial HERA run at reduced collision energy, which are particularly sensitive to the contribution of longitudinal structure function F_L at small x [1]. This run was motivated by a particular sensitivity of the small- x F_L to the resummation effects and collinear factorization violation. Besides, F_L is quite sensitive to the gluon distribution therefore the data of Ref. [1] can help to consolidate the small- x gluon distributions provided by different groups, cf. Fig. 1.

In our analysis the DIS data are described within the 3-flavour FFN scheme, as well as in the ABKM09 case. However, in the present fit we employ the heavy-quark Wilson coefficients with the \overline{MS} definition for the c - and b -quark masses, as suggested in Ref. [8]. For the case of \overline{MS} definition the perturbative stability of the calculations is substantially improved. Moreover, in this case the constraints on the heavy-quark masses coming from the e^+e^- data, which are commonly obtained in the \overline{MS} definition, can be consistently imposed in the PDF fit. This leads to a reduction of the PDF uncertainties due to the heavy-quark masses. In particular, the errors in the 4(5)-flavour heavy-quark PDFs, which are generated from the 3-flavour ones using the matching conditions, are significantly improved as compared to the earlier ABKM09 PDFs, cf. Fig. 2.

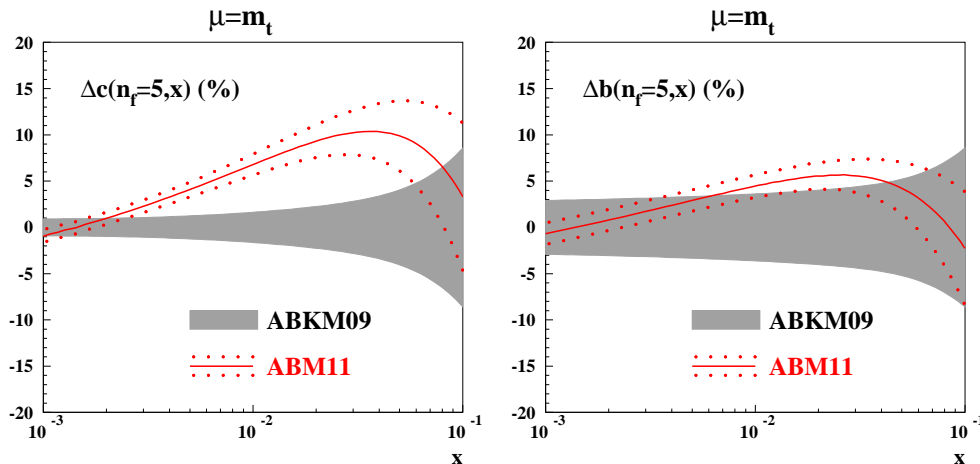


Figure 2: The charm- (left) and the bottom-quark (right) PDFs obtained in the fit: The dotted (red) lines denote the $\pm 1\sigma$ band of relative uncertainties (in percent) and the solid (red) line indicates the central prediction resulting from the fit with the running masses taken at the PDG values [9]. For comparison the shaded (grey) area represents the results of ABKM09 [6].

The value of strong coupling constant $\alpha_s(M_Z)$ is determined in our fit simultaneously with the PDFs. This approach provides a straightforward treatment of their correlation that is important for calculation of the uncertainties in the hadronic cross section predictions. At NNLO the ABM11 fit obtains the value of $\alpha_s(M_Z) = 0.1134 \pm 0.0011(\text{exp.})$. This is comparable with our earlier determination $\alpha_s(M_Z) = 0.1135 \pm 0.0014(\text{exp.})$ [6], while the error is improved due to more accurate data employed in the present analysis. It is also in a good agreement with $\alpha_s(M_Z) = 0.1141^{+0.0020}_{-0.0022}$ obtained in the analysis of the non-singlet DIS data with account of the QCD corrections up to the $N^3\text{LO}$ [10]. In the ABM11 analysis the value of α_s is constrained both by the non-singlet and the singlet DIS data, cf. Fig. 3. For the kinematics of the SLAC and NMC experiments the χ^2 -profile is sensitive to the power corrections including target

mass effects and the dynamical twist-4 terms. The latter are poorly defined by the strong interaction theory and therefore put limit on the accuracy of α_s determined in our fit. On the other hand, the BCDMS and HERA data are insensitive to the power term due to kinematics peculiarities. Moreover, these data sets provide complementary constraints in determining α_s [11]. Performing the NNLO variant of our fit with the SLAC and NMC data dropped we obtain $\alpha_s(M_Z) = 0.1133 \pm 0.0011(\text{exp.})$, which is not affected by the power corrections. Furthermore, it is in nice agreement with one obtained in the nominal ABM11 fit that gives confidence in the consistent treatment of the power terms in our analysis (cf. also discussion in Ref. [12]).

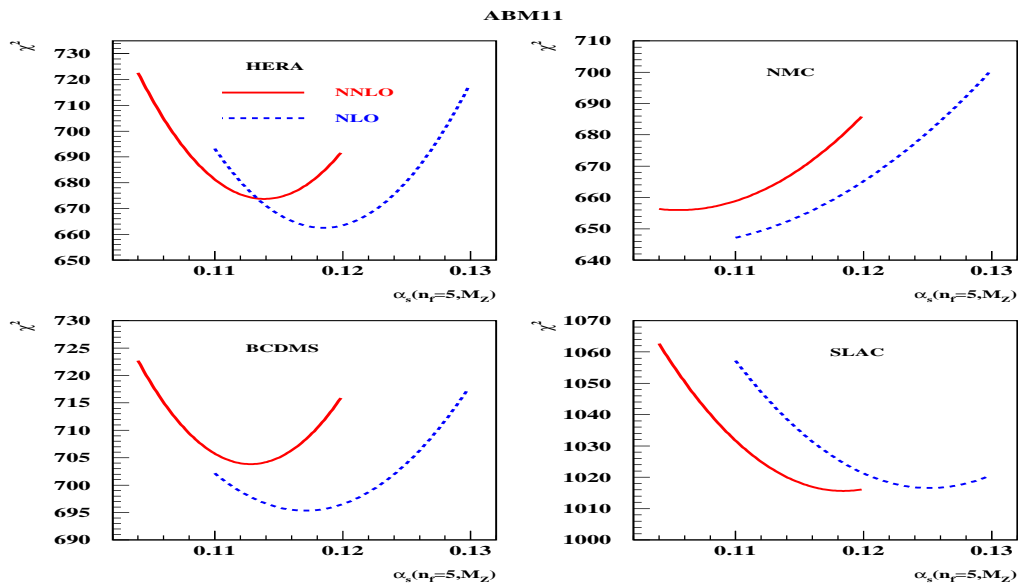


Figure 3: The χ^2 -profile versus the value of $\alpha_s(M_Z)$, for the separate data subsets, all obtained in variants of the present analysis with the value of α_s fixed and all other parameters fitted (solid lines: NNLO fit, dashes: NLO fit).

Predictions for the charged-lepton asymmetry and the inclusive jet production cross sections at the energy of LHC are in a good agreement with the first data collected by the CMS and ATLAS experiments [13, 14, 16, 15], cf. Figs. 5, 4, despite these data are not used in ABM11 fit. Moreover, the value of $\alpha_s = 0.1151 \pm 0.0001(\text{stata.}) \pm 0.0047(\text{sys.})$ extracted from the ATLAS data of Ref. [16] in the NLO [17] is in agreement with our results. In contrast, the jet Tevatron data go above our predictions and the large- x gluon distribution rises significantly once they are included in the analysis. Note that the MSTW PDFs systematically overshoot the LHC jet data (cf. Fig. 5) as well as other PDFs tuned to the Tevatron data [15, 16]. On the whole, this leads to the conclusion that the LHC data prefer softer gluons as compared to the Tevatron case.

The Higgs production rates at the LHC and Tevatron are widely defined by the gluon distribution shape and the value of α_s . The NNLO predictions for the cross section of Higgs production in the proton-proton collisions at the LHC energies calculated with different NNLO

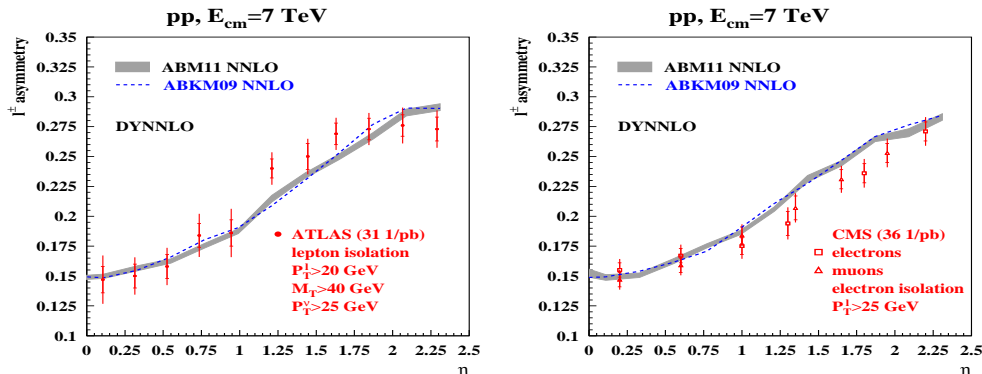


Figure 4: The data on charged-lepton asymmetry versus the lepton pseudo-rapidity η obtained by the ATLAS [13] (left panel) and CMS [14] (right panel) experiments compared to the NNLO predictions based on the DYNNLO code [18] and the ABM11 NNLO PDFs with the shaded area showing the integration uncertainties. The ABKM09 NNLO predictions are given for comparison by dashes, without the integration uncertainties shown.

PDFs are displayed in Table . At smaller collision energy, when the production rate is more sensitive to the large- x gluon distribution tail, the ABM11 calculations go lower than the MSTW08 and NN21 ones, while at high energies the difference between the predictions is smaller.

\sqrt{s} (TeV)	ABM11	ABKM09 [6]	JR09 [2, 19]	MSTW08 [3]	NN21 [20]
7	$13.23^{+1.35+0.30}_{-1.31-0.30}$	$13.12^{+1.34+0.38}_{-1.31-0.38}$	$13.02^{+1.24+0.41}_{-1.17-0.41}$	$14.39^{+1.54+0.17}_{-1.47-0.22}$	$15.14^{+1.68+0.21}_{-1.53-0.21}$
8	$16.99^{+1.69+0.37}_{-1.63-0.37}$	$16.87^{+1.68+0.47}_{-1.63-0.47}$	$16.53^{+1.54+0.53}_{-1.44-0.53}$	$18.36^{+1.92+0.21}_{-1.82-0.28}$	$19.30^{+2.09+0.26}_{-1.89-0.26}$
14	$44.68^{+4.02+0.85}_{-3.78-0.85}$	$44.75^{+4.07+1.16}_{-3.85-1.16}$	$42.13^{+3.60+1.59}_{-3.26-1.59}$	$47.47^{+4.52+0.50}_{-4.18-0.71}$	$49.77^{+4.91+0.54}_{-4.30-0.54}$

Table 1: The total NNLO cross sections in pb for Higgs production in the gluon-gluon fusion obtained with different PDF sets at the mass of Higgs boson $M_H = 125$ GeV. The errors shown are the scale uncertainty are based on the shifts $\mu = m_H/2$ and $\mu = 2m_H$ and the 1σ PDF uncertainty, respectively.

In summary, we have produced the new NNLO PDF set with improved accuracy at small x due to new input from the HERA data and refined theoretical treatment of the heavy-quark electro-production in the running-mass definition. The predictions based on these PDFs are in a good agreement with the first LHC data, which can be used in future to improve the PDF accuracy further. A benchmarking w.r.t. to other PDFs is performed; the differences found can be also reduced with the help of new HERA and LHC data.

References

- [1] F. Aaron, C. Alexa, V. Andreev, S. Backovic, A. Bagdasaryan, *et al.* Eur.Phys.J. **C71** (2011) 1579, arXiv:1012.4355 [hep-ex].
- [2] P. Jimenez-Delgado and E. Reya. Phys.Rev. **D79** (2009) 074023, arXiv:0810.4274 [hep-ph].

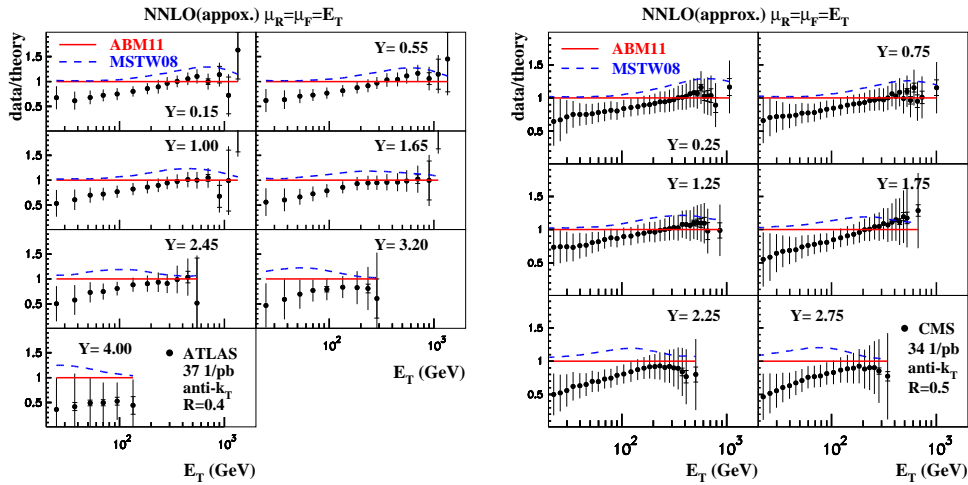


Figure 5: Cross section data for 1-jet inclusive production from the ATLAS collaboration [16] (left panel) and from the CMS collaboration [15] (right panel) as a function of the jets transverse energy E_T for $\mu_R = \mu_F = E_T$ compared to the result of the present analysis (solid) and to MSTW [3] (dashed). The theory predictions include the NNLO threshold resummation corrections to the jet production.

- [3] A. Martin, W. Stirling, R. Thorne, and G. Watt. *Eur.Phys.J.* **C63** (2009) 189–285, [arXiv:0901.0002](#) [[hep-ph](#)].
- [4] R. D. Ball, V. Bertone, F. Cerutti, L. Del Debbio, S. Forte, *et al.* *Nucl.Phys.* **B849** (2011) 296–363, [arXiv:1101.1300](#) [[hep-ph](#)].
- [5] S. Alekhin, J. Blümlein, and S. Moch. [arXiv:1202.2281](#) [[hep-ph](#)].
- [6] S. Alekhin, J. Blumlein, S. Klein, and S. Moch. *Phys.Rev.* **D81** (2010) 014032, [arXiv:0908.2766](#) [[hep-ph](#)].
- [7] F. Aaron *et al.* *JHEP* **1001** (2010) 109, [arXiv:0911.0884](#) [[hep-ex](#)].
- [8] S. Alekhin and S. Moch. *Phys.Lett.* **B699** (2011) 345–353, [arXiv:1011.5790](#) [[hep-ph](#)].
- [9] K. Nakamura *et al.* *J.Phys.G* **G37** (2010) 075021.
- [10] J. Blumlein, H. Bottcher, and A. Guffanti. *Nucl.Phys.* **B774** (2007) 182–207, [arXiv:hep-ph/0607200](#) [[hep-ph](#)].
- [11] C. Adloff *et al.* *Eur.Phys.J.* **C21** (2001) 33–61, [arXiv:hep-ex/0012053](#) [[hep-ex](#)].
- [12] S. Alekhin, J. Blumlein, and S. Moch. *Eur.Phys.J.* **C71** (2011) 1723, [arXiv:1101.5261](#) [[hep-ph](#)].
- [13] G. Aad *et al.* *Phys.Lett.* **B701** (2011) 31–49, [arXiv:1103.2929](#) [[hep-ex](#)].
- [14] S. Chatrchyan *et al.* *JHEP* **1104** (2011) 050, [arXiv:1103.3470](#) [[hep-ex](#)].
- [15] S. Chatrchyan *et al.* *Phys.Rev.Lett.* **107** (2011) 132001, [arXiv:1106.0208](#) [[hep-ex](#)].
- [16] G. Aad *et al.* *Phys. Rev.* **D86** (2012) 014022, [arXiv:1112.6297](#) [[hep-ex](#)].
- [17] B. Malaescu and P. Starovoitov. [arXiv:1203.5416](#) [[hep-ph](#)].
- [18] S. Catani, L. Cieri, G. Ferrera, D. de Florian, and M. Grazzini. *Phys.Rev.Lett.* **103** (2009) 082001, [arXiv:0903.2120](#) [[hep-ph](#)].
- [19] P. Jimenez-Delgado and E. Reya. *Phys.Rev.* **D80** (2009) 114011, [arXiv:0909.1711](#) [[hep-ph](#)].
- [20] R. D. Ball *et al.* *Nucl.Phys.* **B855** (2012) 153–221, [arXiv:1107.2652](#) [[hep-ph](#)].